Numerical Calculation of the Charge Density Distribution in a Gas Discharge Field of an Electron Beam Printhead

Hiroyuki Kawamoto and Shin-ichiro Serizawa

Foundation Research Laboratory, Corporate Research Laboratories, Fuji Xerox Co., Ltd., 430 Sakai, Nakai-machi, Ashigarakami-gun, Kanagawa 259-01, Japan

Numerical calculations were performed to simulate charging characteristics of an electron beam printhead. Because the electric conduction in the gas discharge field is determined not only by electrostatic potential but also by ionic or electronic charge density, two coupled partial differential equations, the continuity equation of charge and Poisson's equation, were numerically solved by the finite-element method under the boundary condition that the electric field at a discharge electrode is a constant determined by a corona starting electric field strength. It was demonstrated that the calculated portion of the high charge density corresponds to the observed luminous and highly degraded portion. The calculation also confirmed that predominant charging particles on the printhead are not ions but electrons. The present method can be utilized for practical design of the charging process.

Journal of Imaging Science and Technology 41: 629–632 (1997)

Introduction

A charging process using gas discharge devices is one of the most important subsystems in electrophotography,[1] ionography,[2,3] and electron beam printing systems.† [4–7] A corotron[1] has been the most widely used charger for electrophotography, and a contact charger roller[8–10] was recently developed and applied for a low-speed electrophotography machine. An electron beam printhead is another charge device that directly forms electrostatic latent image dots on a dielectric coated drum. Calculation of the charge density distribution is key to the design because not only charging characteristics but also degradation of the photoreceptor and the discharge electrode[11,12] are highly affected by charge density. Many mathematical models[13–17] have been developed in attempts to clarify how charger performance is affected by parameters of the charger and the charging system. However, reported applications of the proposed mathematical models have been only for electrophotography and no numerical investigation has been conducted for the electron beam printhead.

In this report, the space charge field in the electron beam device was calculated by the finite element method. Calculated results were compared with experimental evidence, and the numerical method was utilized to clarify the charging mechanism and to improve the performance of the system.

Modeling

Because electric conduction in a gas discharge field is determined not only by the electrostatic potential ϕ but also by the ionic or electronic charge density ρ, two coupled partial differential equations govern the unipolar fields.[13,17]

$$\nabla(-\omega\rho\nabla\phi) = 0 \quad \text{(continuity equation of charge)}, \tag{1}$$

$$-\varepsilon_0\nabla^2\phi = \rho \qquad \text{(Poisson's equation)}, \tag{2}$$

where ε_0 is the permittivity of free space and ω is the mobility of ions or electrons. Here, diffusion and convection of charged particles are neglected. Boundary conditions with respect to the potential are derived from the fact that the potential difference between the gas discharge and collecting electrodes is equal to the applied voltage ϕ_0.

$$\begin{aligned} \phi &= \phi_0 \text{ at the discharge electrode,} \\ \phi &= 0 \text{ at the collecting electrode.} \end{aligned} \tag{3}$$

But because the boundary condition for the charge density is not known, it is assumed in this model that the electric field strength at the surface of the discharge electrode is kept at a constant value E_0 equal to the calculated electrostatic field strength determined by the measured corona starting voltage in a coaxial electrode configuration.[13]

$$E = -\nabla\phi = E_0\,(=14.55\times10^6\ \text{V/m}) \text{ at the discharge electrode.} \tag{4}$$

Numerical Method

The procedure of the numerical method is (1) two differential equations corresponding to the charge continuity and Poisson's equation are solved with respect to ϕ by the finite element method with an initial guess of ρ; (2) distributions of the electric field strength, E_A and E_B, corresponding to

† A non-impact printing system developed and commercialized by Delphax (Mississauga, Ontario, Canada) used to be called "ionography," because it had been believed that *ions* generated by a printhead formed a dot matrix latent image on a dielectric coated drum. However, after it was discovered that primarily *electrons* produce the latent image,[18] the term "electron beam" has been used for this printing system. The charging printhead is one of the most important components in the electron beam printer.

Original manuscript received March 7, 1997

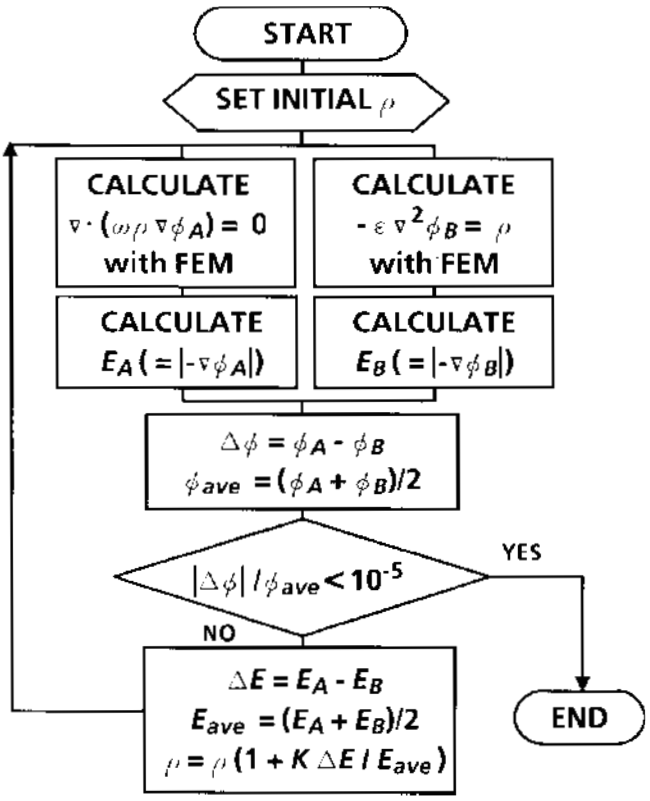

Figure 1. Flowchart of numerical method.

two calculated potential distributions, ϕ_A and ϕ_B, are calculated separately; and (3) the calculations are repeated with the revised charge density distribution $\rho_i = \rho_{i-1}(1 + K\,\Delta E/E_{ave})$ ($\Delta E \equiv E_A - E_B$, $E_{ave} \equiv (E_A + E_B)/2$, K; relaxation coefficient, 0.3 ~ 0.9), until $2|\phi_A - \phi_B|/(\phi_A + \phi_B) < 10^{-5}$ everywhere, where A and B indicate the charge continuity and Poisson's equations, respectively. Figure 1 shows a flowchart of the numerical method. The adequacy of the method was confirmed by comparing numerical solutions with analytical and experimental ones in a coaxial cylindrical field.[13]

Results and Discussion

The present method was applied to simulate charging characteristics of the ion beam printhead shown in Fig. 2. When high voltage is applied between drive and control electrodes separated by a dielectric glass layer, the air is ionized at the edge of the control electrode facing the drive electrode. Charged particles are accelerated by the electric field between the control electrode and a drum to form dot matrix electrostatic images on the surface of the dielectric coated drum. A full-length head consists of several thousand dots. The distance between adjacent dots is about 800μm. An insulating layer made of glass prevents discharge between adjacent control electrodes. Electrostatic potential between the control and screen electrodes controls electron extraction, which is print or non-print of the latent image. Electrons are injected to the drum through holes in the screen electrode. The control electrode is the discharge electrode, and the drum corresponds to the collecting electrode in the condition of image printing, and in turn, the screen electrode is the collecting electrode under non-print condition. The head was manufactured in our laboratory by means of thick film technology.[19] The control and screen electrodes are made of nickel and stainless steel, respectively.

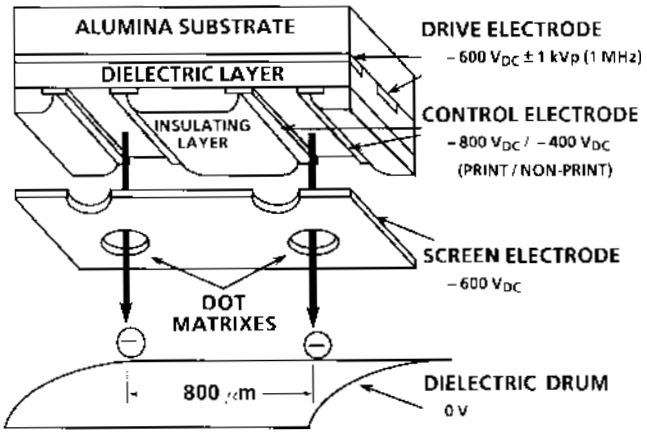

Figure 2. Schematic drawing of electron beam printhead. Although a multiplexing scheme is employed in a full-length printhead, a cut model with two dots is schematically shown in the figure.

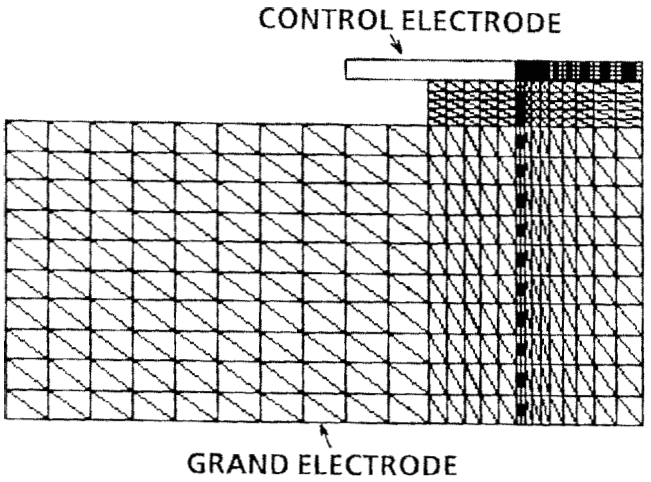

Figure 3. Mesh pattern for numerical calculation using the finite element method.

Because the system is too small to measure the electrostatic potential or charge density distribution directly, simulation is useful to improve the system. Figure 3 shows the mesh pattern for the finite element method. The system is assumed two-dimensional, and according to the symmetricity, one half of the dot is selected as a calculation domain. Figure 4(a) is the electrostatic potential distribution without gas discharge ($\rho = 0$) and Fig. 4(b) is with gas discharge.

Careful comparison of these two figures allows us to deduce the well-known characteristic that gas discharge relaxes the field concentration in the vicinity of the discharge electrode. Figure 4(c) shows the charge density distribution calculated simultaneously with the potential distribution shown in Figure 4(b). Clearly, charge density is high at the edge of the control electrode and the surface of the dielectric layer corresponding to the observed luminous (Fig. 5) and highly degraded (Fig. 6) parts. Figure 5 shows luminescence of the gas discharge. The luminous part corresponds to the screen-toned part of Fig. 1 and the most luminous two parallel lines correspond to the edges of the control electrode. This experimental observation supports the adequacy of the calculation, and it

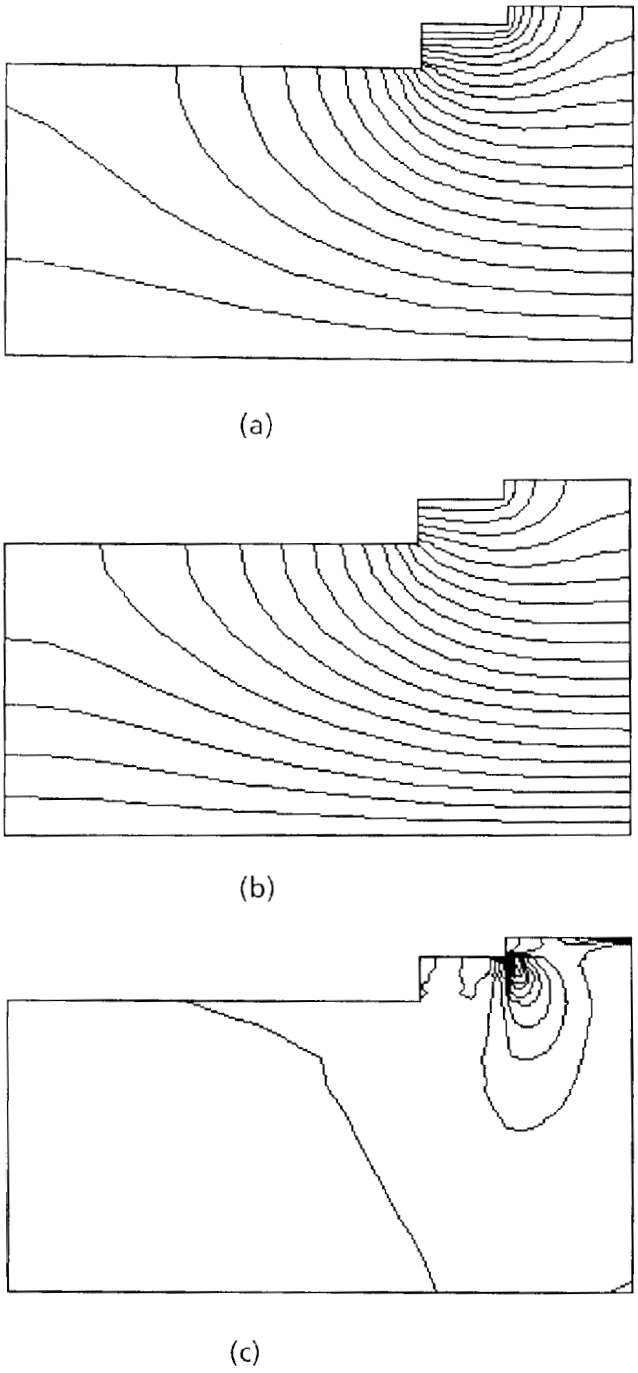

Figure 4. Calculated distribution of electrostatic potential and charge density. (a) Electrostatic potential distribution without discharge ($\rho = 0$), (b) electrostatic potential distribution under discharge operation, and (c) charge density distribution.

is particularly noteworthy that although the boundary condition of the calculation did not assume the gas discharge at the surface of the dielectric layer, calculated charge density was self-consistently large at this surface. Note also that the edges of the control electrode were highly degraded as shown in Fig. 6, taken after 150 h of operation. Silicon oxide, one of the most predominant gas discharge products,[11,12] was formed at the degraded parts. Formation of SiO_2 at the control electrode edges changes output current, and degradation of the dielectric layer results in dielectric breakdown.

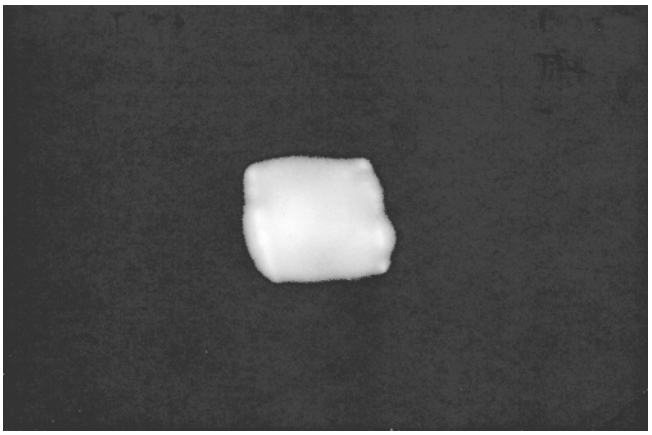

Figure 5. Luminescence during discharge.

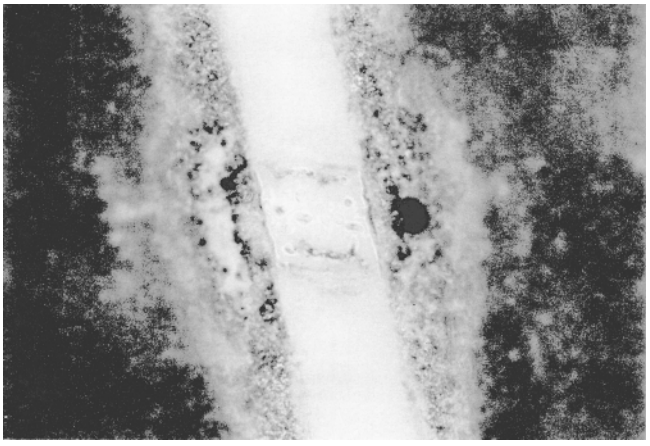

Figure 6. Degraded printhead after 150 h of operation.

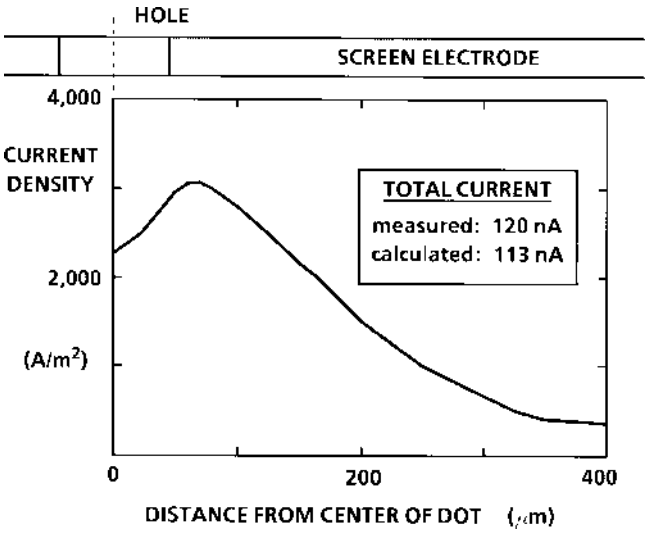

Figure 7. Distribution of current flowing into the collecting electrode.

Figure 7 shows the distribution of current flowing into the collecting electrode. The calculated total current using electron mobility 0.08 m^2/Vs was 113 nA/dot, which agreed well with the measured value 120 nA/dot. When ion mobility 1.9×10^{-4} m^2/Vs is used to derive the total current, it is more than 400 times smaller than the measured.

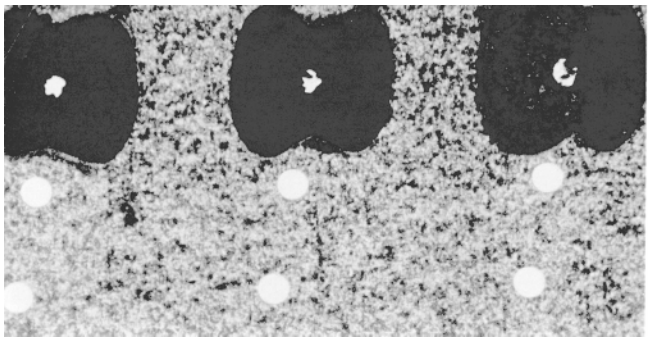

Figure 8. Screen electrode. The upper row of three dots were operated for 150 h and the lower allowed no current passage. The area of the hole was reduced by corrosion, and this resulted in decrease of the output current injected to the drum.

The calculation and the experiment confirm that the predominant charging particles in this system are not ions but electrons.[18] Another piece of information deduced from Fig. 7 is that the current density is high near the edge of a screen electrode hole. This calculated result also coincides with experimental evidence that the screen electrode becomes highly corroded at the edge of the hole as shown in Fig. 8.

Although direct comparison of the distribution of the charge density in this microdevice is impossible, these results justify the adequacy of the present simulation method. This method can be utilized for the practical design of the discharge device and the process.

Acknowledgments. The authors wish to thank T. Tanaka, T. Yamada, K. Udagawa, Y. Kurosawa, and S. Hirosaki for conducting out experiments.

References

1. R. M. Schaffert, *Electrophotography* (Focal Press, MA, 1975).
2. N. K. Sheridon, *Proc. SPIE*, **1252,** 25 (1990).
3. R. G. Stearns, G. W. Bowers, N. K. Sheridon, M. S. Bernstein, R. T. Fulks, M. Hack, H. C. Tuan, L. E. Fennel, J. C. Mikkelsen, Jr. and R. Matusiak, *Proc. SPIE*, **1252,** 33 (1990).
4. J. R. Rumsery and D. Bennewitz, *J. Imaging Technol.* **12**, 144 (1986).
5. R. A. Fotland, *Proc. SPIE*, **1252,** 19 (1990).
6. E. B. Devitt, *Proc. SPIE*, **1252,** 67 (1990).
7. R. G. Stearns, *Proc. SPIE*, **1252,** 77 (1990).
8. J. Araya, N. Koitabashi, S. Nakamura and H. Hirabayashi, GM. Patent 280 542 (1988).
9. J. Araya, N. Koitabashi, S. Nakamura and H. Hirabayashi, US Patent 5,164,779 (1992).
10. H. Kawamoto and H. Satoh, *J. Imaging Sci. Technol.* **38,** 383 (1994).
11. K. Nashimoto, *Japan J. Appl. Phys.* **26,** L1138 (1987).
12. K. Nashimoto, *Japan J. Appl. Phys.* **27,** L1181 (1988).
13. M. Hattori and K. Asano, *Trans. IEE Japan*, **106-A,** 95 (1986), in Japanese.
14. Y. Watanabe, *Proc. Inst. Electrostat. Jpn.* **14,** 494 (1990) in Japanese.
15. Y. Watanabe, K. okada, M. Sato and S. Namekata, *Electrophoto.* **30,** 439 (1991) in Japanese.
16. H. Myochin, Y. Inoue and J. Okuno, *Electrophoto.* **31,** 53 (1992) in Japanese.
17. H. Igarashi, S. Sasaki, T. Nakamura and T. Honma, *IEEE Trans. Mag.* **29,** 1508 (1993).
18. J. Calery, Jr., W. R. Buchanan and T. W. Pape, *J. Imaging Sci. Technol.* **147,** 51 (1991).
19. C. A. Harper, *Handbook of Thick Film Hybrid Microelectronics* , McGraw-Hill, 1982.